Multiple Energy Scaling of Blast Waves from Heterogeneous Explosives

Jeff Leadbetter[1], Robert C. Ripley[1], Fan Zhang[2], David L. Frost[3]

[1]Martec Limited, 1888 Brunswick St., Suite 400, Halifax, Nova Scotia, B3J3J8 Canada

[2]Defence R&D Canada – Suffield, PO Box 4000, Stn Main, Medicine Hat, Alberta, T1A8K6 Canada

[3]McGill University, Mechanical Engineering Department, Montreal, Quebec, H3A2K6 Canada

1 Introduction

Free-field blast scaling of heterogeneous explosives containing reactive metal particles involves multiple length-scales, as opposed to Sach's classic scaling which is based on a single length scale (cubic root of total explosion energy) [1]. After detonation, late-time energy release occurs when explosively-dispersed particles react in the detonation products and surrounding air. Systematic experiments involving magnesium and aluminum particles of varying diameters have found that for a given particle size, there exists a critical charge diameter for particle ignition (CDPI) above which a prompt uniform reaction of the dispersed particle cloud occurs and significantly influences the blast [2-3]. Previously, a preliminary blast scaling study of these charges was performed using a single energy scale $R_0 = (E_0/4\pi\gamma p_0)^{1/3}$ where E_0 is the total explosion energy including energy of detonation and energy from complete oxidation of metal particles in air [4]. When this simple scaling was applied to experimental data from spherical nitromethane charges containing aluminum particles and with charge diameters above CDPI, the results showed the scaled data in a scatter band below Sach's scaling curve for homogenous explosives. In the present work, a multiple length-scale model is further introduced by investigating the energy partitions and blast scaling associated with length scales using numerical simulations.

2 Multiple energy scaling concept

When a spherical charge consisting of a condensed explosive mixed with reactive metal particles detonates, the energy available for the blast wave is considered to be partitioned into three regimes: energy of the explosive detonation (E_0), anaerobic metal particle combustion with detonation products (E_1), and expanding aerobic metal particle combustion with air (E_2). The energy release time scale for E_0 (t_0) is the detonation time scale. The effective energy release time scale for E_1 ($t_1 > t_0$) is assumed to correspond to the expansion of the fireball to the first maximum radius (R_1) above which the fireball will not provide any positive work to drive the blast. Similarly, the effective energy release time scale for E_2 ($t_2 > t_1$) is assumed to correspond to a maximum expansion radius (R_2) for particle reaction front with a critical particle concentration limit. Beyond R_2, the particle reaction is quenched by the gas flow or provides little contribution to the blast.

The energy-scaling rule for the heterogeneous blast can then be obtained in a modified Sach's form:

$$R_0 = \left(\frac{E_0 + E_1 + E_2}{(4\pi\gamma) p_0} \right)^{\frac{1}{3}} \tag{1}$$

Where R_0 is the constant factor used to scale blast results, p_0 is the initial pressure of the surrounding air, and γ is the isentropic coefficient. Values of E_1, E_2, E_3, for use with Equation 1 are taken at their respective time scales, t_0, t_1, t_2.

According to the energy-scaling principle, Equation 1 is valid in the far field. At near-field radii comparable to length scales R_1 and R_2 associated with E_1 and E_2, deviation from Equation 1 is expected due to the extra length scales involved. The corresponding energy release timescales, t_1 and t_2, are rate dependent because of finite particle heating and burning rates which depend on particle diameter.

Experimentally, a CDPI upper limit is defined above which a prompt uniform reaction of the expanding particle cloud is observed [2-3]. Theoretically, the residence time of particles within the detonation products must overcome the expansion cooling of the products so that the particles can react within the products. Since E_1 must be obtained from the reaction of particles within the products, Equation 1 is only valid for charge diameters larger than the CDPI upper limit.

Correspondence to: fan.zhang@drdc-rddc.gc.ca

3 Numerical simulation results

The numerical model employs a two-phase Eulerian solver and a diffusion-based particle reaction model [5]. The fluid phase utilizes a constant reaction time model for the nitromethane detonation, and a JWL equation of state is used for detonation products. As air temperature is critically important to particle heating and reaction, a variable gamma ideal gas law utilizing NASA CEA thermodynamic data is employed. Tracer gases, independent of the flow solver are used to monitor evolution and distribution of oxidising gas species and their reaction with metal particles. Convective heat transfer and momentum transfer (drag) between phases is simulated using empirical correlations. Additionally, early stage momentum transfer resulting from detonation interaction with the particles is modeled using an adjustment factor to account for the highly dense particle flow [6]. Charge diameters range from 9.3 cm to 250 cm, corresponding to a mass range of 0.889 kg to 16,700 kg. Aluminum particles catalogued by Valimet Ltd. as H-10 (d_p = 13 µm) and H-50 (d_p = 54 µm) were employed in the calculations, and particle mass fractions in charges followed the experiments in [2-4].

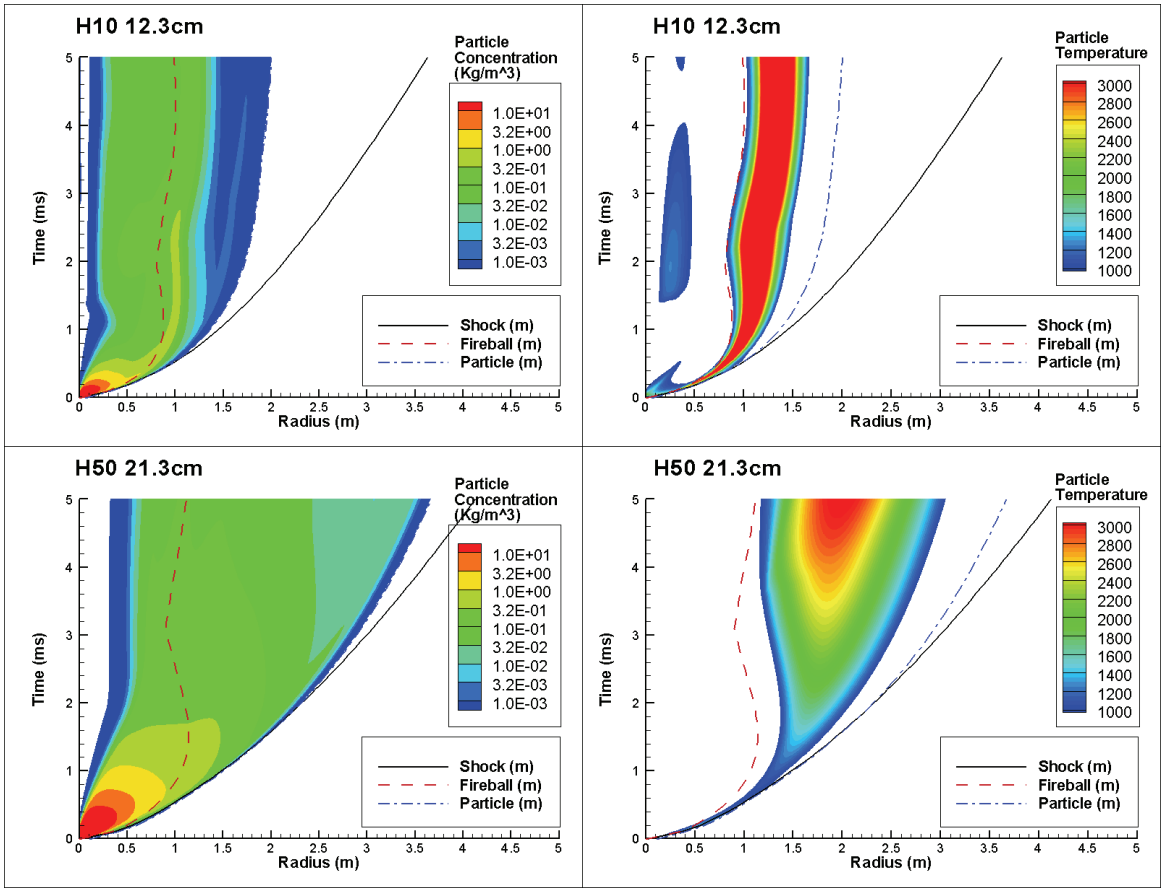

Figure 1. *x-t* diagrams of particle concentration (left), and particle temperatures above 933 K (right).

Figures 1 and 2 show the three length scale concept of centrally-initiated spherical charges containing H-10 and H-50 particles. Particle dispersal dynamics are elucidated on the left of Figure 1 using particle concentration levels, while combustion behaviour is shown on the right of Figure 1 using temperature levels (particle combustion occurs in the presence of oxidizers for $T_p > 933$ K). In Figure 2, the reaction history is shown using the spatially integrated masses of particles and oxidizers. For the 12.3 cm charge with H-10, $R_1 \approx 0.9$ m and $R_2 \approx 1.6$ m, beyond which particle combustion in air is quenched by the cool gas flow. Particle combustion within the detonation products takes place promptly, while particles that penetrate the products interface burn continuously in the shocked air. The termination of particle combustion in the products is due to the complete consumption of H_2O and CO_2 within less than 100 µs as shown in Figure 2. For the 21.3 cm charge with H-50 particles, $R_1 \approx 1.2$ m and $R_2 \approx 3.0$ m, and as displayed in Figures 1 and 2, the residence time of particles within the detonation products is not sufficient to overcome the expansion cooling of the products, hence the larger particles do not react within the products. Particles that penetrate the products interface are heated and react in the shocked air.

Spatial integration of the results is used to determine E_0, E_1 and E_2, where distinction between E_1 and E_2 was achieved by recording the amount of H_2O and CO_2 consumed in the detonation products (anaerobic) and the

amount of O_2 remaining (aerobic), respectively. Figure 3 (left) shows the partitioning of detonation (E_0), anaerobic (E_1), and aerobic (E_2) combustion energies. For H-10 particles, considerable E_1 (20% of total) is released in the early time for 9.3 cm charges (also see Figures 1-2). For H-50 particles, a comparable amount of E_1 is released only when the charge diameter exceeds 50 cm, while for charge diameters of 21.3 cm or less particle combustion occurs only in the shocked air (partially due to slight over-prediction of temperature from the air equation of state). According to the similarity of energy partition shown in Figure 3, a correlation $D \sim d_p^n$ (where D is charge diameter and d_p is particle diameter) with $n \approx 1.5$ can be obtained and one can conclude that the CDPI upper limit is 9.3 cm for H-10 particles and about 75 cm for H-50 particles when assuming a threshold $E_1/(E_0+E_1+E_2) = 0.2$. Figure 3 (left) also indicates that an increase in charge diameter results in an increase in partitioning of E_1 and a decrease in E_2. As shown on the right of Figure 3 considerable particles are un-reacted within the detonation products, due to complete consumption of H_2O and CO_2, and in the air due to cooling from the gas flow.

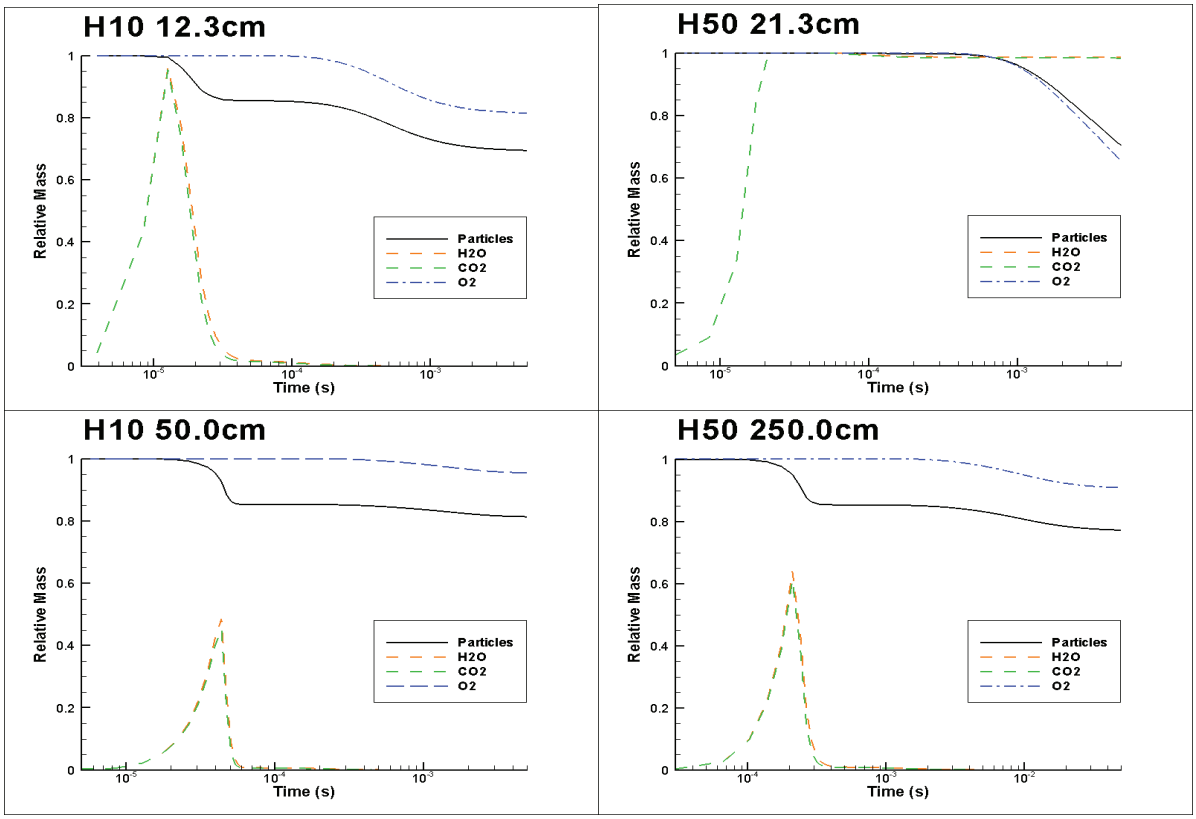

Figure 2. Reaction history of spatially integrated particle mass and oxidizer masses.

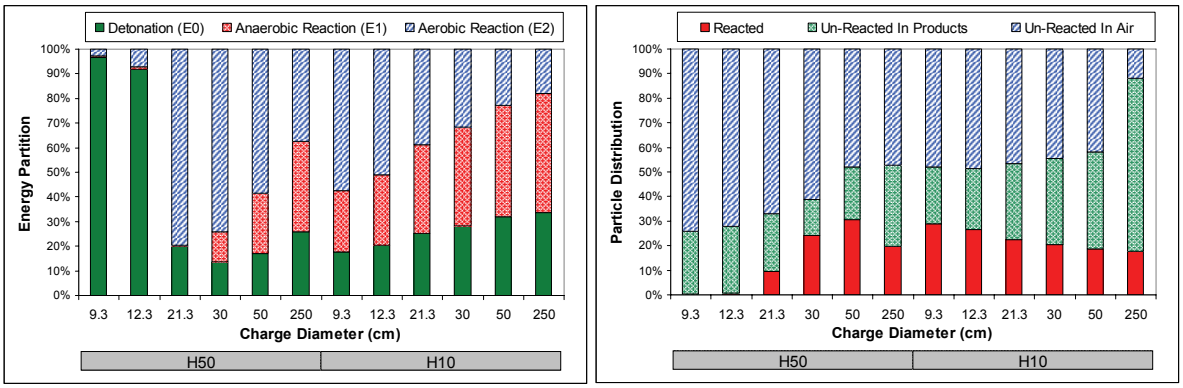

Figure 3. Energy partition at anaerobic burning time t_1 for $E_0 + E_1$ and aerobic burning time t_2 for E_2 (left), and particle mass partition for burned and unburned particles in the products and air (right).

Figure 4 shows Sach's scaling (upper figures) using total energy $E_0 + E_{2max}$, where E_{2max} is the energy from the oxidation of all metal particles [4], and scaling using Equation 1 (lower figures). The scaling using $E_0 + E_{2max}$

displays a scatter band of data which lies below Sach's scaling curve for homogenous explosives. In contrast, the scaling using Equation 1 shows data collapse except for H-50 particles with charge diameters below 50 cm. Apart from the effect of limited length scales (R_1 and R_2) in the near field, the smaller charges with H-50 produce little particle combustion in the detonation products as the charge diameter is less than the CDPI upper limit. For these charges, late time particle combustion in the air does not contribute to the blast front, but does add to the positive phase of the impulse. The conclusions achieved in this work indicate the qualitative nature of the multiple length-scale heterogeneous blast. Quantitative prediction needs to be studied further; this is challenged by development of aluminum particle ignition and combustion models under extreme explosion flow conditions.

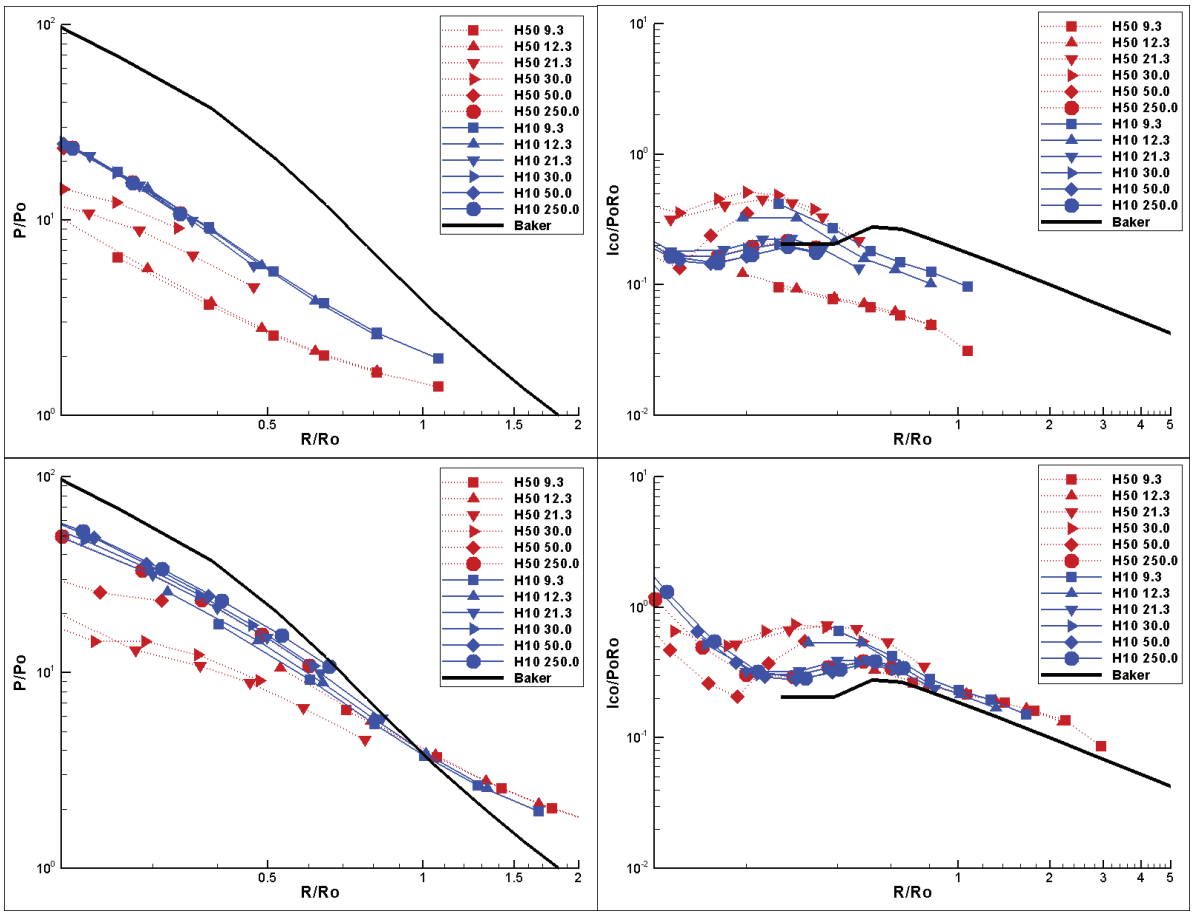

Figure 4. Heterogeneous blast scaling using: total energy $E_0 + E_{2,max}$ (top), and partitioning energies from Equation 1 (bottom).

References

[1] Baker WE (1973). Explosions in Air. University of Texas Press, Austin

[2] Frost DL, Zhang F, Murray SB, McCahan S (2002). Critical conditions for ignition of metal particles in a condensed explosive. Proceedings of 12th International Detonation Symposium, San Diego, CA

[3] Frost DL, Goroshin S, Ripley RC, Zhang F (2006). Effect of Scale on the Blast Wave from a Metalized Explosive. 13th International Detonation Symposium, Norfolk, VA

[4] Frost DL, Zhang F (2006). The Nature of Heterogeneous Blast Explosives. 19th International Symposium on Military Aspects of Blast and Shock, Calgary, Alberta

[5] Zhang D, Frost DL, Thibault PA, Murray SB (2001). Explosive Dispersal of Solid Particles. Shock Waves 10: 431-443

[6] Ripley RC, Zhang F, Lien FS (2006). Detonation Interaction with Metal Particle in Explosives. 13th International Detonation Symposium, Norfolk, VA